Novel G Protein-Coupled Oestrogen Receptor GPR30 Shows Changes in mRNA Expression in the Rat Brain over the Oestrous Cycle

Emma J. Spary   Sally E. Chapman   John K. Sinfield   Azhar Maqbool   Jean Kaye
Trevor F.C. Batten

Division of Cardiovascular and Neuronal Remodelling, LIGHT Institute, University of Leeds, Leeds, UK

Abstract

Oestrogen influences autonomic function via actions at classical nuclear oestrogen receptors α and β in the brain, and recent evidence suggests the orphan G protein-coupled receptor GPR30 may also function as a cytoplasmic oestrogen receptor. We investigated the expression of GPR30 in female rat brains throughout the oestrous cycle and after ovariectomy to determine whether GPR30 expression in central autonomic nuclei is correlated with circulating oestrogen levels. In the nucleus of the solitary tract (NTS), ventrolateral medulla (VLM) and periaqueductal gray (PAG) GPR30 mRNA, quantified by real-time PCR, was increased in proestrus and oestrus. In ovariectomised (OVX) rats, expression in NTS and VLM appeared increased compared to metoestrus, but in the hypothalamic paraventricular nucleus and PAG lower mRNA levels were seen in OVX. GPR30-like immunoreactivity (GPR30-LI) colocalised with Golgi in neurones in many brain areas associated with autonomic pathways, and analysis of numbers of immunoreactive neurones showed differences consistent with the PCR data. GPR30-LI was found in a variety of transmitter phenotypes, including cholinergic, serotonergic, catecholaminergic and nitrergic neurones in different neuronal groups. These observations support the view that GPR30 could act as a rapid transducer responding to oestrogen levels and thus modulate the activity of central autonomic pathways.

Copyright © 2012 S. Karger AG, Basel

Introduction

Neurones throughout the central nervous system (CNS) can be exposed to oestrogen crossing the blood-brain barrier from the circulation or generated locally in the brain by aromatase enzyme activity [1], resulting in various genomic and more rapid, non-genomic effects [2]. Studies on male and female rats clearly demonstrate that direct application of oestrogen in brainstem autonomic centres elicits significant changes in autonomic tone and baroreflex function [3–5]. These centres include the nucleus of the solitary tract (NTS), concerned with coordination and integration of sensory afferent inputs, including those from the cardiovascular system, and the ventrolateral medulla (VLM), which contains the pressor (sympathetic) and depressor (parasympathetic) autonomic output neurones sited in the rostral VLM (RVLM)

Dr. Emma J. Spary
Division of Cardiovascular and Neuronal Remodelling
LIGHT Institute, Worsley Building
University of Leeds, Leeds LS2 9JT (UK)
Tel. +44 113 343 4172, E-Mail E.J.Spary @leeds.ac.uk

and nucleus ambiguus (NAmb), respectively [6, 7]. These medullary autonomic nuclei are influenced by descending projections from higher brain regions containing oestrogen receptive neurones, including hypothalamic areas, such as the paraventricular nucleus (PVN) and the midbrain periaqueductal gray (PAG) [6, 8–10]. The actions of oestrogen in these multiple brain areas, which interact to determine autonomic outflow, may contribute to coordinating physiological and behavioural changes associated with reproductive cycles. Moreover, there is a considerable body of evidence showing that changes in the levels of circulating oestrogen that occur over the oestrous cycle and following ovariectomy are correlated to variations in baroreflex function, blood pressure (BP) and heart rate (HR) [11–14].

The diverse effects of oestrogen are elicited via oestrogen receptors (ERs). Transcriptional effects are mediated by two isoforms of 'conventional' ER – ERα and ERβ – which have been localised to cell nuclei in several brain areas involved in autonomic regulation [15]. The possibility that other plasma membrane-associated ERs might be implicated in a wide variety of neural and extraneural targets of oestrogen action has received much debate, since specific binding sites for oestrogen were described at the outer surface of isolated endometrial cells [16]. One such membrane receptor is an orphan G protein-coupled receptor GPR30 [17, 18], which mediates oestrogen's rapid actions via second messenger signalling pathways. However, there is still some debate over GPR30's cellular localisation as it has been proposed as an intracellular transmembrane ER at the endoplasmic reticulum but was also reported in electron microscopic immunohistochemical studies to be present at the plasma membrane of CA2 pyramidal neurones [19].

The distribution of GPR30 immunoreactivity in adult rat brain has already been described, identifying cells in the hypothalamic PVN and supraoptic nuclei, hippocampus, substantia nigra and pituitary [20–22]. In the medulla oblongata, GPR30-immunoreactive cells were noted in areas involved in autonomic control, including the area postrema, the NTS, the dorsal vagal nucleus (DVN) and NAmb [20, 23]. The expression of conventional ERs is reported to alter over the rat oestrous cycle in response to fluctuations in circulating oestrogen [24–27], but while GPR30 expression levels are related to the oestrous cycle in the hamster ovary [28], similar changes in GPR30 expression in the CNS have not been investigated.

This study uses quantitative real-time PCR and immunohistochemistry to investigate GPR30 expression in the rat brain and to assess changes in expression of this putative cytoplasmic ER over the oestrous cycle and following ovariectomy. We explore whether the resultant fluctuations in circulating oestrogen levels have effects on GPR30 expression in a number of brain areas recognised as contributing to the control of autonomic function. Our working hypothesis was that expression of GPR30, like ERα, might be influenced by circulating levels of oestrogen, which could indicate a functional role in mediating rapid actions of oestrogen on the central neural networks responsible for initiating cardiovascular responses, with possible implications for post-menopausal cardiovascular disease.

Preliminary data from this study was presented at the 5th Congress of the International Society of Autonomic Neuroscience (ISAN) in Kyoto, October 5–8, 2007 [29].

Methods

Adult (12- to 14-week-old) Wistar male (200–250 g) and virgin female (200–250 g) rats were supplied by University of Leeds Central Biomedical Services and bilaterally ovariectomised (OVX) rats (200–280 g) were supplied by Harlan. Age-/weight-matched sham-operated females underwent a similar surgical procedure but without ovary removal. All rats were housed in groups of 4 with 12-hour light/dark cycles (lights on 06:00 h) with free access to food and water and were left for 3 weeks following surgery. Oestrous cycle stages of intact females were monitored for 2 weeks prior to experimentation by microscopic analysis of vaginal smear exfoliative epithelia taken twice daily at 10:00–11:00 h and 15:00–16:00 h, and only those exhibiting a regular 4- to 5-day cycle were used. Oestrous cycle stages were identified as metoestrus (lowest circulating oestrogen levels), dioestrus, proestrus (highest circulating oestrogen levels) and oestrus. Procedures for tissue collection and perfusion fixation were performed under anaesthesia (5% halothane in >95% O_2) between 11:00 and 13:00 h done in accordance with the regulations of the UK Animals (Scientific Procedures) Act, 1986.

Tissue Collection
Rats were killed by decapitation and blood samples collected for 17β-oestradiol assay using an ELISA kit (Cayman Chemicals: 582251). Oestrous stages and ovariectomy were confirmed at this point. Brains were removed, rapidly frozen on dry ice and coronal slices of 0.5–1 mm thickness were cut from the brainstem. Tissue punches were collected using a 0.69-mm corer under a ×5 dissecting microscope from the hypothalamus, PAG, NTS and VLM. In addition, samples were taken from individual areas of the hypothalamus including the PVN, the lateral hypothalamic area (LH) and the arcuate (Arc), dorsomedial (DMH) and ventromedial (VMH) nuclei. Placement of the medullary punches was confirmed as previously described [30].

RNA Extraction and PCR
Total RNA was isolated (SV Total RNA extraction system; Promega) and reverse transcribed as described previously [27]. PCR

was performed using GeneAmp Fast PCR Master Mix (Applied Biosystems) with 1–2 μl of first-strand product as a template, in a GeneAmp Fast 9800 thermocycler (Applied Biosystems), with 0.4 μM subtype-specific GPR30 primers (forward 5′-TGGCTGCAA-CTACTCCAGCA-3′, reverse 5′-CGTGGTGCTTGGTGCGGAA-3′). Amplification was performed using parameters established previously [27] and products separated on 2% agarose gels containing ethidium bromide visualised under UV light. PCR products were confirmed by DNA sequencing on an ABI 3130XL genetic analyser using BigDye terminator cycle sequencing version 3.1. Negative controls included amplification of RNA (without reverse transcription) and water.

Real-Time PCR (qPCR)

Real-time PCR was performed on an ABI7500 system using Applied Biosystems TaqMan gene expression assays for rat GPR30 (Rn00592091_s1) in a MicroAmp 96-well optical plate as described previously [27]. Expression levels were normalised to rat β-actin (Rn00667869_m1) performed in parallel as an endogenous control, as this showed no variation in expression between samples. Results were analysed using the comparative $2^{-\Delta\Delta C_T}$ method where C_T is the cycle threshold number. All results were expressed relative to metoestrus (low oestrogen) values, which were normalised to 100%. Data are shown as mean ± SEM. Statistical significance was determined using ANOVA followed by Bonferroni's multiple comparison test, with significance accepted at $p < 0.05$.

Perfusion Fixation

Adult rats (n = 3 for each phase of the cycle and OVX) were perfused via the transcardial route with 200 ml Ames' medium (Sigma-Aldrich), then 500 ml 4% paraformaldehyde in 0.1 M phosphate buffer. Brains were post-fixed for 2 h in 4% paraformaldehyde, then stored in phosphate-buffered saline (PBS), pH 7.6. Coronal 50-μm sections were cut on a vibrating microtome (VT 1000S; Leica Microsystems) and collected serially in a 24-well tissue culture plate (Costar-Corning) containing PBS.

GPR30 Antibody

This study used a rabbit antibody raised against a synthetic peptide mapping the C-terminal of the human GPR30 sequence, which shares 94% homology and identity with the rat sequence (NLS4272; Novus Biologicals). This antibody, used at 1/1,000 dilution (1 μg/ml), is known to recognise GPR30 from a range of species including rodents and human. The specificity of the antibody was tested by preabsorption for 24 h at 4°C with 5 μg/ml of two commercially available C-terminal peptides (Novus Biological and Santa Cruz).

Immunofluorescence Labelling

Free-floating sections were labelled by a standardised procedure as described previously [27], with bound GPR30 antibodies visualised with a species-specific Cy3-conjugated anti-rabbit IgG (1/1,000; Jackson ImmunoResearch/Stratech Scientific). To identify the anatomical location and phenotype of structures labelled for GPR30, double fluorescence labelling was performed by simultaneously incubating sections with GPR30 antibody and antibodies to a number of different neurochemical markers: neuronal nitric oxide synthase (NOS) raised in sheep (1/10,000; gift of P. Emson), vasopressin (VP, guinea pig; 1/2,000; Peninsula Labs), choline acetyltransferase (ChAT; goat; 1/1,500; Chemicon), tyro-

sine hydroxylase (TH; mouse; 1/4,000; ImmunoStar) and 5-hydroxytryptamine (5-HT; rat clone YC5/45; 1/1,000; Abcam). Mouse monoclonal antisera to glial fibrillary acidic protein (GFAP; 1/500; Affiniti Research Products), vimentin (VIM; clone V9; 1/2,000; Sigma) and ERα (ID5 clone; 1/100; Dako) were also used for dual labelling, as were antibodies to the following protein markers for specific intracellular compartments: transferrin receptor (TNFR; mouse; 1/500; Invitrogen) for endoplasmic reticulum; trans-Golgi network membrane protein (TGN38; sheep; 1/800; Serotec) for the Golgi system; lysosome-associated membrane protein (LAMP1; mouse; 1/1,000; Stressgen) for lysosomes. Sections were incubated in a mixture of species-specific secondary antibodies conjugated to Cy3 and to biotin (1/500; Jackson) for 2 h. The binding of the neuronal marker antibodies was visualised with streptavidin-Alexa[488] (1/1,000; Molecular Probes). Secondary antibody specificity was established by the absence of labelling on sections incubated with normal rabbit serum in place of primary antibody, and the species specificity was confirmed by tests on sections incubated with primary antibodies raised in an inappropriate species.

After washing in PBS, sections were mounted in Vectashield (Vector Labs) and examined on an AxioImager.Z1 microscope (Carl Zeiss) fitted with appropriate filter sets. Images were captured and processed with the Axiovision imaging system, including 'Apotome' confocal imaging and 'colocalisation' modules.

Quantitative Immunohistochemical Analysis

The numbers of neurones labelled by GPR30 antibodies per unit volume of tissue in defined brain regions was estimated using a three-dimensional counting method based on the 'optical dissector' and adapted for use on stacks of confocal images through thick sections [27]. The brain regions analysed were the PVN at 4 levels of sectioning from bregma –1.9 to –1.25 mm [31]; the PAG at 4 levels from –5.4 to –8.0 mm [32]; the RVLM at 4 levels from –11.6 to –12.6 mm [32], and the medial subnucleus of NTS at 4 levels from –13.6 to –14.2 mm [32]. To ensure consistent positioning of areas sampled in sections through these regions, alternate sections were dual labelled with antibodies to NOS and TH (or VP for the PVN). In the case of the PAG, ventrolateral and dorsolateral zones were analysed separately. Stacks of confocal images were captured at 1-μm z-steps through a 20- to 30-μm depth of the section using the ×20 objective and Apotome illumination and labelled cells were counted as previously described [27]. Numbers of cells displaying double labelling were counted and expressed as a percentage of GPR30-positive neurones and NOS-, TH- or VP-positive neurones. All counts were performed blindly by a single observer, and only neuronal profiles displaying a continuous ring of immunoreactive cytoplasm around an unlabelled nucleus were included.

Results

Expression of the GPR30 mRNA in the Rat Brain over the Oestrous Cycle

Plasma oestrogen concentrations measured using ELISA showed that levels increased from metoestrus (13.36 ± 2.66 pg/ml) to dioestrus (23.63 ± 2.34 pg/ml), then peaked during proestrus (42.35 ± 0.26 pg/ml) before decreasing
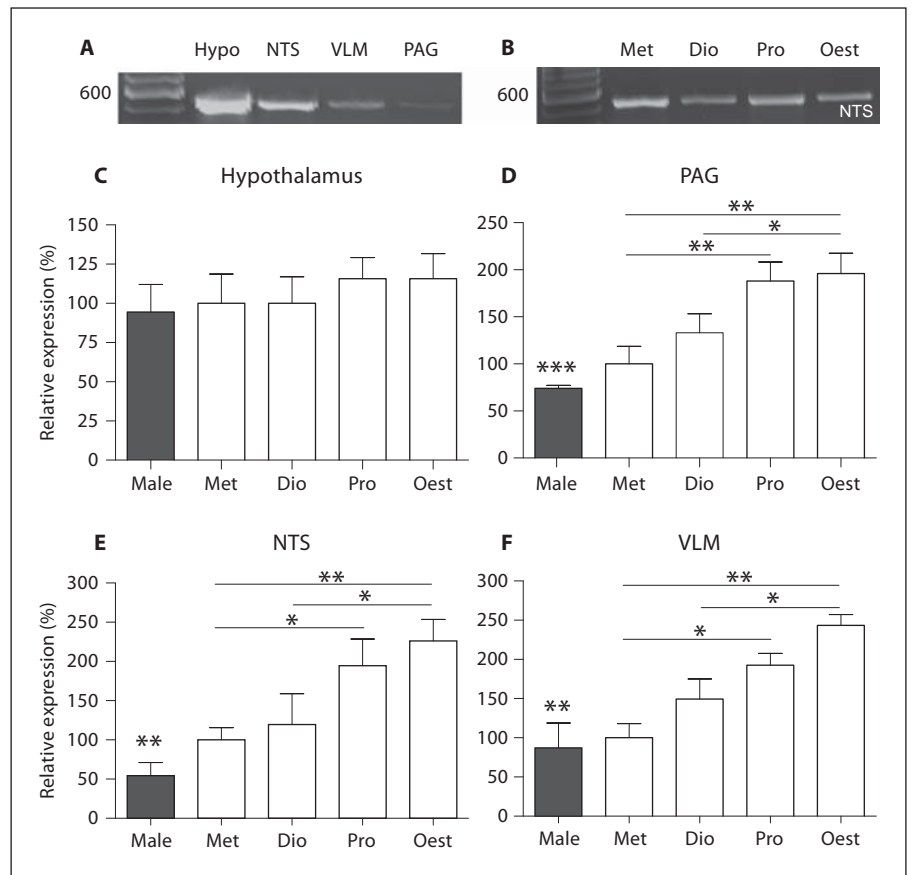
Fig. 1. Changes in GPR30 mRNA expression levels over the oestrous cycle. **A** GPR30 PCR products (520 bp) were separated on 2% agarose gels stained with ethidium bromide (n = 6). GPR30 was detected in the hypothalamus (Hypo), nucleus of the solitary tract (NTS), ventrolateral medulla (VLM) and periaqueductal gray (PAG) in both male and female animals (shown here in the male). **B** Amplicons were present at each stage of the oestrous cycle, metoestrus (Met), dioestrus (Dio), proestrus (Pro) and oestrus (Oest) (shown here in the NTS). **C–F** Relative expression of GPR30 mRNA was measured using real-time PCR (n = 6 of each), normalised to a β-actin internal control. All results were compared to metoestrus, which has been normalised to 100%. Results shown are the mean ± SEM and differences analysed by an ANOVA with Bonferroni's post-hoc test. In the hypothalamus (**C**) GPR30 levels showed little variation between the oestrous stages. In the PAG (**D**), NTS (**E**) and VLM (**F**) the levels of GPR30 increased throughout the cycle with significantly higher levels in proestrus compared to metoestrus (* $p < 0.05$, ** $p < 0.01$), and oestrus compared to both metoestrus (** $p < 0.01$) and dioestrus (* $p < 0.05$). In all three areas the levels in the male animal were significantly decreased compared to oestrus (** $p < 0.01$, *** $p < 0.001$).

in oestrus (12.80 ± 1.10 pg/ml). PCR analysis was performed on cDNA samples taken from the hypothalamus, PAG, NTS and VLM at each of the 4 stages of the oestrous cycle and from male rats (n = 6, each group). GPR30 mRNA was expressed in all the areas tested (fig. 1A) and was present at each stage of the oestrous cycle, as shown in the NTS (fig. 1B). The veracity of the PCR products was confirmed by DNA sequencing. No amplification products were detected in the negative control reactions.

Real-time PCR on males (n = 6) and females (n = 6 per oestrous phase) performed on tissue taken from the hypothalamus, PAG, NTS and VLM revealed variations in GPR30 expression across the oestrous cycle. In general, the level of expression in the male animals was lower than that in the females with significantly lower levels in the PAG ($p < 0.001$), NTS ($p < 0.01$) and VLM ($p < 0.01$) compared to oestrus (fig. 1). Levels of GPR30 mRNA expression in the hypothalamus showed little variation between the oestrous stages (fig. 1C). In the PAG (fig. 1D) significantly higher levels of GPR30 mRNA were observed in proestrus ($p < 0.01$) and oestrus ($p < 0.01$) compared to metoestrus, and in oestrus compared to dioestrus (p <
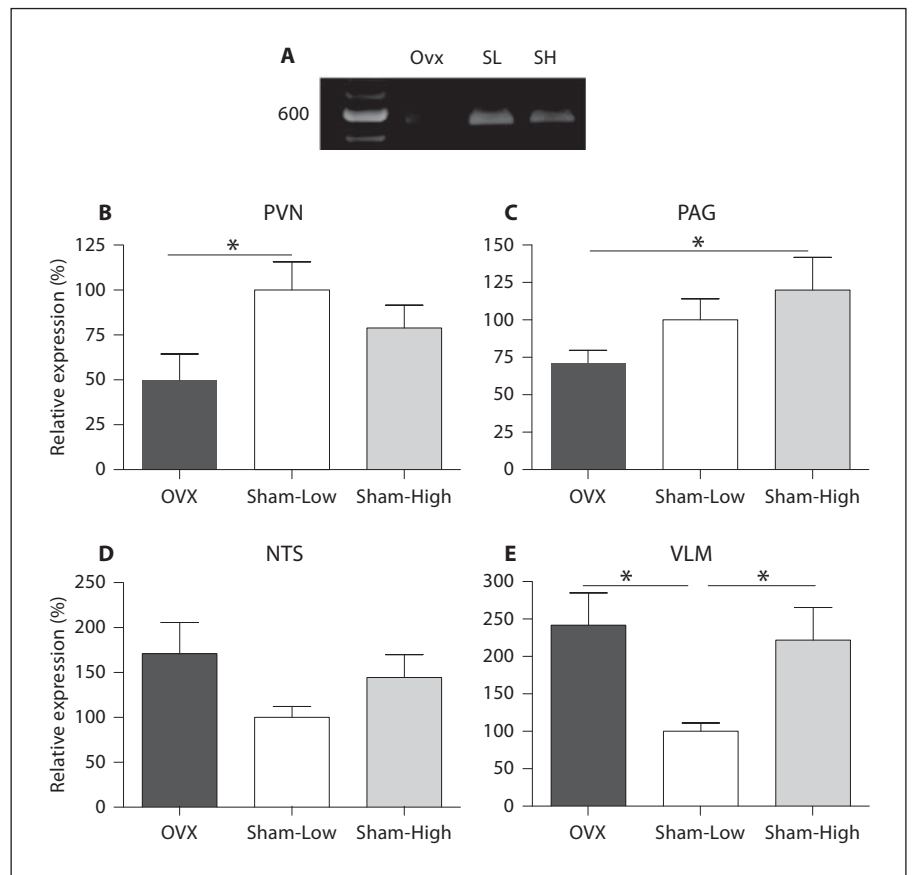
Fig. 2. Changes in GPR30 expression following ovariectomy. In the ovariectomised females (OVX) and the sham-operated controls sampled during low oestrogen phases (SL) and high oestrogen phases (SH) GPR30 was detected in the hypothalamus, NTS, VLM and periaqueductal gray (PAG) (shown here in the NTS (**A**)). Relative expression of GPR30 mRNA was measured in OVX female rats and sham-operated animals sampled during met/dioestrus (Sham-Low) and proestrus (Sham-High) using real-time PCR (n = 6 of each), normalised to a β-actin internal control. All results were compared to the sham-operated animals sampled in met/dioestrus (Sham-Low), which has been normalised to 100%. Results shown are the mean ± SEM and differences analysed by an ANOVA with Bonferroni's post-hoc test. In the PVN (**B**) and PAG (**C**), decreased GPR30 mRNA levels were seen following ovariectomy compared to the sham-operated controls (PVN * $p < 0.05$ vs. metoestrus, PAG * $p < 0.05$ vs. proestrus). The decrease in the PVN (**B**) was significantly lower (* $p < 0.05$) compared to the sham animals sampled in metoestrus (Sham-Low). In the NTS (**D**) and VLM (**E**) increased GPR30 mRNA expression was observed in the OVX animals, with significantly higher levels in the VLM (**E**) of the OVX compared to the sham animals in metoestrus (* $p < 0.05$).

0.05). Analysis of the NTS (fig. 1E) and VLM (fig. 1F) revealed a similar result with the expression of GPR30 significantly increased in proestrus ($p < 0.05$) compared to metoestrus, and oestrus compared to both metoestrus ($p < 0.01$) and dioestrus ($p < 0.05$).

Expression of the GPR30 mRNA in the Rat Brain following Ovariectomy

Expression levels in tissue samples from OVX rats were compared with those from sham-operated females during metoestrus (low oestrogen) and proestrus (high oestrogen) phases (n = 6 each group). PCR analysis revealed GPR30 mRNA expression in the LH, Arc, PVN, DMH, VMH, PAG, NTS (fig. 2A) and VLM of each group, confirmed by DNA sequencing.

Real-time PCR showed that expression levels of GPR30 in the sham-operated animals were comparable to the levels observed in the intact females, confirming that the sham operation had no effect on GPR30 expression. In the LH, Arc, DMH and VMH, GPR30 mRNA expression levels in the OVX females were not significantly different to those observed in both groups (high
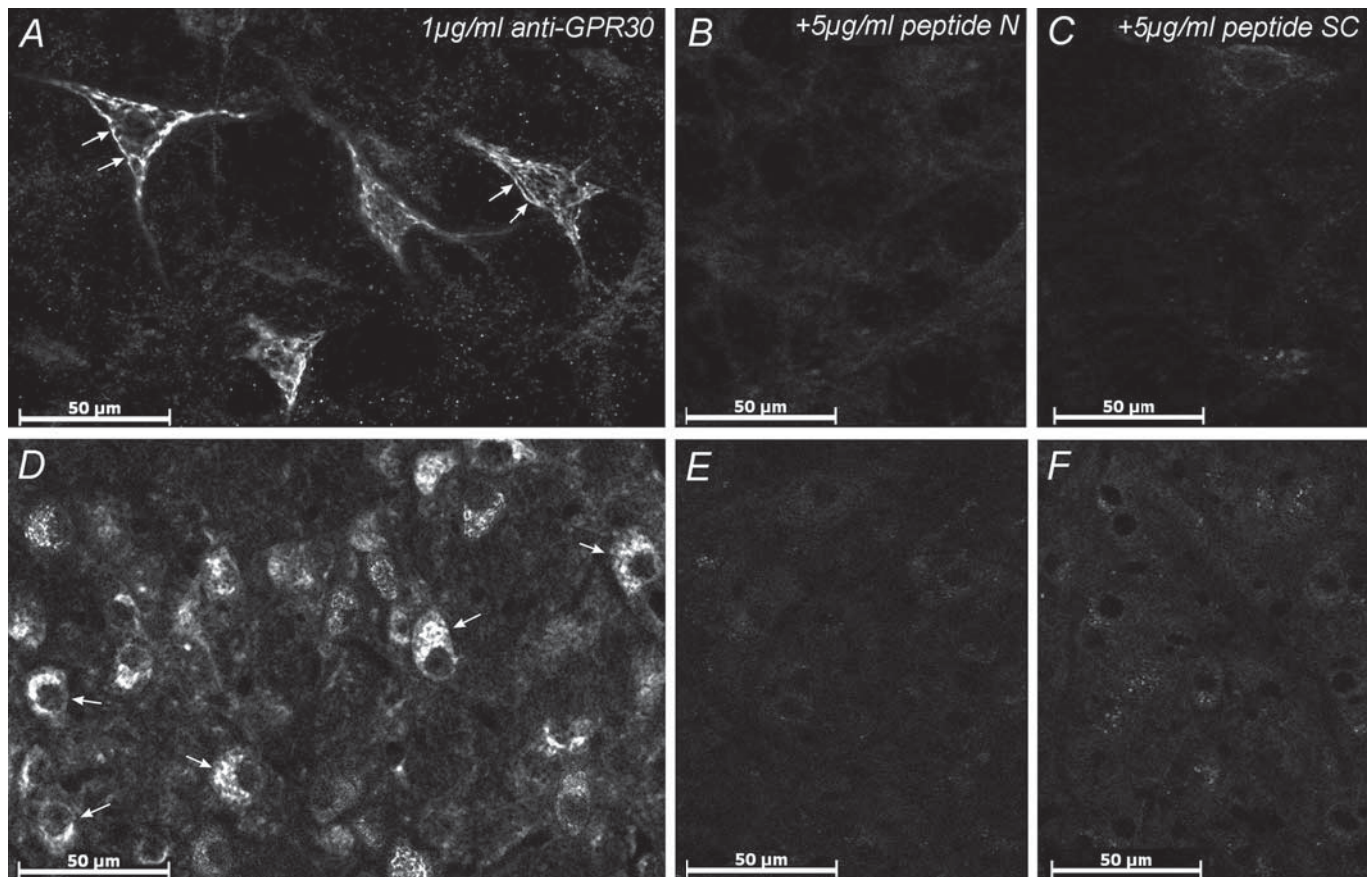
Fig. 3. Specificity test of GPR30 antiserum. Confocal images of similar areas of the brain in serial sections of the medulla oblongata incubated with the working dilution of GPR30 antiserum (**A**, **D**) and antiserum preabsorbed with two different C-terminal peptides (**B**, **E** and **C**, **F**), using identical Cy3 labelling protocols and imaging parameters. **A** shows gigantocellular neurones of the ventromedial medulla with intense intracellular GPR30-LI with-in the cytoplasm and proximal dendrites, with some labelling underlying the plasmalemma (arrows). **D** shows smaller neurones of the rostral NTS with less intense, more homogeneous labelling. In both cases, immunoreactivity is abolished by the antigenic (Novus, N) peptide (**B**, **E**) and only faintly detectable in a few neurones by preabsorption with a similar but non-homologous (Santa Cruz, SC) peptide (**C**, **F**). Scale bars = 50 μm.

Fig. 4. Distribution and colocalisation of GPR30-LI in the forebrain. For each group of confocal images, the insets (**A1**, **A2**, etc.) show single red (GPR30) and green channel images and the larger images (**A**, **B**, etc.) show the merged channels. Scale bars indicate 50 μm, except for **B**, **G** and **I**, 20 μm. **A** Hypothalamic paraventricular nucleus (PVN), showing GPR30-LI colocalisation in a subpopulation of vasopressin (VP)-immunoreactive neurones (arrows). **B** GPR30-LI is absent in most strongly NOS-immunoreactive neurones of the PVN, but detectable in some of the less intensely NOS-positive neurones (arrows). **C** In the arcuate nucleus and periventricular hypothalamus, GPR30-LI is colocalised in a few catecholaminergic neurones (arrows). **D** GPR30-LI neurones in the ventral hypothalamus are distinct from those with nuclei expressing ERα, as shown in the ventromedial nucleus (VMH). **E** In the posterodorsal thalamus, cells with intense GPR30-LI are distinct from the NOS-positive neurones of the precommis-sural nucleus (PrC). **F** Lateral wall of the mammillary recess of the third ventricle (3V), showing small GPR30-positive cells (arrows) in the dorsal premammillary nucleus (PMD) and intermingled with tanycyte-like ependymal cells labelled by vimentin (VIM) antibodies in the arcuate nucleus (Arc). **G** GPR30-LI in cells and puncta within the subfornical organ (SFO), with apparent colocalisation in NOS-immunoreactive cells (arrows). **H** Strong GPR30 labelling in the subcommissural organ (SCO), with ependymal cells and astrocytes labelled by antibodies to glial fibrillary acidic protein (GFAP). Note clusters of small GPR30-positive cells (arrows) at the lateral margin of the SFO beneath the posterior commissure (pc). **I** Similar patterns of immunoreactivity within a thalamic PrC neurone dual labelled for GPR30 and trans-Golgi protein TGN38, thus indicating an intracellular localisation mainly within the Golgi system.

Spary/Chapman/Sinfield/Maqbool/Kaye/
Batten

4

and low oestrogen phases) of sham animals (not shown). Analysis of tissue taken from the PVN (fig. 2B) revealed significantly less GPR30 mRNA in the OVX animals compared to the sham females sampled during metoestrus (p < 0.05). GPR30 mRNA levels also appeared to be lower in the PAG of the OVX animals compared to both the sham groups (p < 0.05 OVX vs. proestrus) (fig. 2C). In contrast, in the medullary nuclei, the NTS and VLM (fig. 2D, E), the levels of expression of GPR30 mRNA were greater in OVX females compared to the controls (VLM, p < 0.05 OVX vs. sham-low).
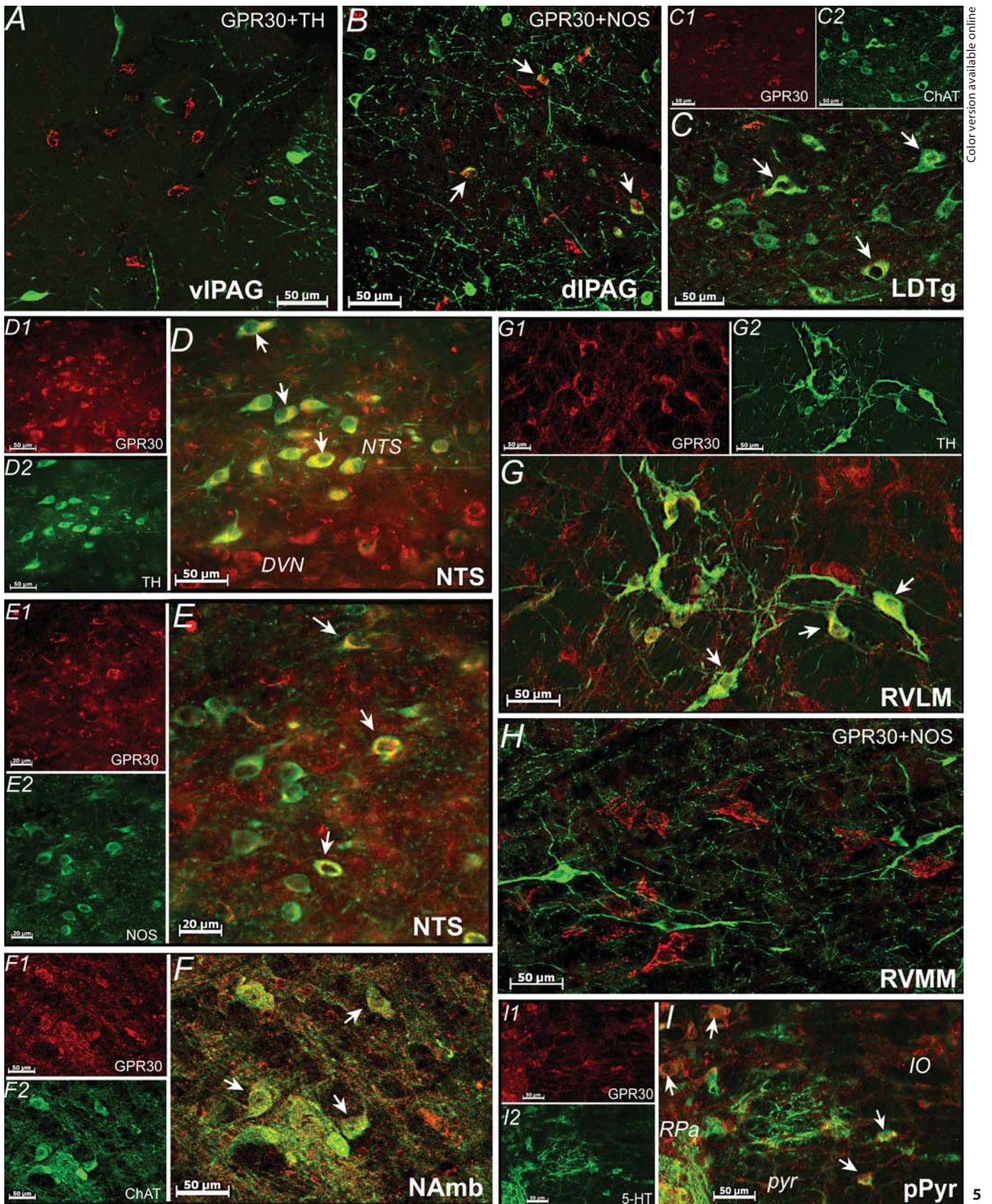
Immunohistochemical Localisation of GPR30

GPR30-like immunoreactivity (GPR30-LI) was present in neurones of many anatomical divisions of the brain, but these displayed a rather variable appearance. GPR30-positive neurones were often intensely labelled, with GPR30-LI apparently outlining a network of membranes or cisternae within the cytoplasm of the soma and proximal dendrites, in some cases closely associated with the plasmalemma (fig. 3A). We refer to this as the intensely labelled type of GPR30 neurone. Other, more numerous neurones displayed a less intense, more homogeneous immunoreactivity within their cytoplasm (fig. 3D). Immunoreactivity was abolished by preabsorption of the antiserum with C-terminal peptides (fig. 3B, C and E, F). The extensive colocalisation with TGN38 immunoreactivity suggested that this pattern of labelling represented expression predominantly within the Golgi apparatus (fig. 4I). On the other hand, intracellular GPR30-LI was distinctly different from both TNFR1 and LAMP1 immunoreactivities (not shown). There appeared to be no major differences in the overall pattern of distribution of GPR30-LI within the brains of male, female or OVX female rats.

Hypothalamus

Small immunoreactive neurones of the intensely labelled type referred to above were scattered in the ventral hypothalamus, including the Arc (fig. 4C) and VMH (fig. 4D). These appeared mostly to be distinct from neurones expressing NOS or TH (fig. 4C) and they did not show nuclear expression of ERα (fig. 4D). The PVN contained densely packed neurones of the less intensely labelled type displaying more homogeneous GPR30-LI, with some overlap with populations of neurones expressing VP (fig. 4A) or NOS (fig. 4B), but not with TH (table 1). Quantitative immunohistochemical analysis suggested that the volume density of neurones expressing GPR30-LI was significantly reduced in the PVN of OVX rats compared to females in metoestrus or proestrus, with similar numbers to those found in males (fig. 6A). There was also a reduced proportion of NOS-immunoreactive neurones in the PVN showing GPR30-LI in OVX females compared to both sham-operated groups (table 1). Small cells with GPR30-LI occurred along the walls of the third ventricle, sometimes close to the ependymal layer and were particularly noticeable at the levels of the anterior preoptic recess, median eminence and mammillary recess (fig. 4F). The suggestion of an association with circumventricular organs was reinforced by the conspicuous GPR30-LI in small cells and neuropil in the subfornical organ (SFO) and subcommissural organ (SCO). Scattered GPR30-positive neurones extended from the hypothalamus into the thalamus, where they formed prominent bilateral groups spread across the posterior paraventricular thalamic nucleus (PVP) and precommissural nucleus (PrC). These were distinct from a prominent group of NOS-positive cells in the posterodorsal thalamus (fig. 4E).

Fig. 5. Distribution and colocalisation of GPR30-LI in the mid- and hindbrain. **A** GPR30-LI in the ventrolateral PAG (vlPAG) is present in neurones separate from the A11 cells containing tyrosine hydroxylase (TH) immunoreactivity. Extended focus image computed in Axiovision from a confocal z-stack. **B** In the dorsolateral PAG (dlPAG), most GPR30-positive neurones are not for NOS, but a subpopulation of NOS neurones display GPR30-LI (arrows). Extended focus image. **C** Pontine lateral dorsal tegmental nucleus (LDTg) showing moderate levels of GPR30-LI in some of the ChAT-positive cholinergic neurones (arrows). **D** In the dorsomedial medulla, strong GPR30-LI is present in the TH-positive A2 catecholamine neurones of the NTS (arrows), with GPR30 labelling in the parasympathetic efferent neurones of the DVN. **E** A subpopulation of NOS-positive neurones in the NTS contain GPR30-LI (arrows). **F** ChAT-immunoreactive motoneurones of the IX and X cranial nerves in the compact formation of the nucleus ambiguus (NAmb) contain moderate levels of GPR30-LI. **G** In the rostral ventrolateral medulla (RVLM) many of the TH-positive C1 catecholamine neurones colocalise GPR30-LI (arrows). **H** Strongly GPR30-positive gigantocellular neurones (red) lying among NOS-immunoreactive neurones (green) in the rostral ventromedial medulla (RVMM). Extended focus confocal image. **I** Moderate levels of GPR30-LI are present in some 5-HT-immunoreactive neurones (arrows) of the parapyramidal (pPyr) region, including the nucleus raphe pallidus (RPa). Smaller neurones in the inferior olives (IO) are also GPR30-positive. Pyr = Pyramidal tract. All scale bars = 50 μm.
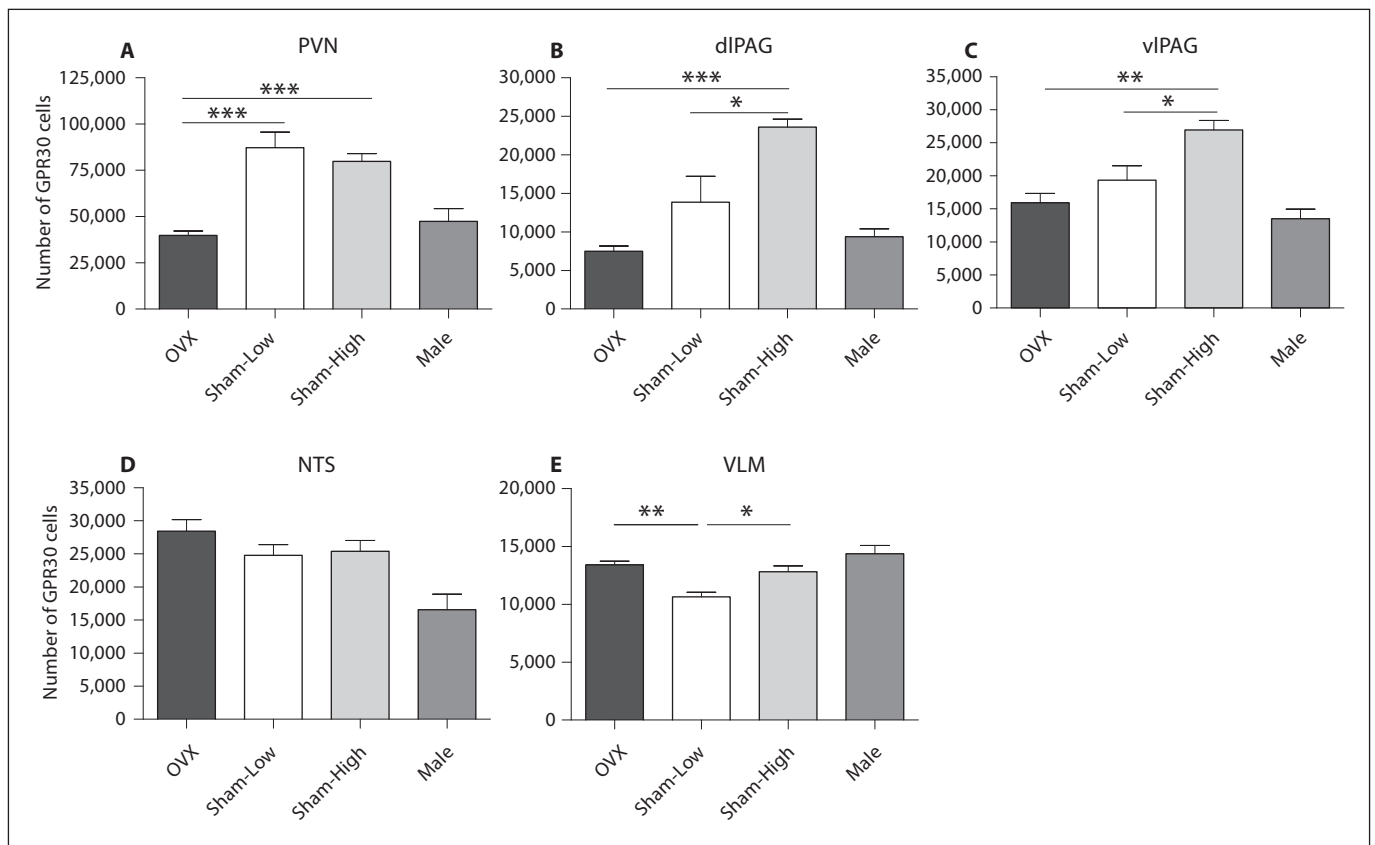
Color version available online

Fig. 6. Number of GPR30-immunoreactive cells counted in autonomic areas of female ovariectomised (OVX), sham-operated and male rats. Sham-operated females were sampled during metoestrus (Sham-Low) and proestrus (Sham-High) assessed by quantitative immunohistochemistry (n = 5 of each). **A** PVN, **B** dlPAG, **C** vlPAG, **D** NTS, **E** RVLM (* $p < 0.05$, ** $p < 0.01$, *** $p < 0.001$).

Midbrain/Pons

Neurones containing GPR30-LI formed discontinuous groups in the ventrolateral and dorsolateral divisions of the PAG (vlPAG and dlPAG). Some of these were of the intensely labelled type, but most showed less intense labelling. They were distinct from any TH-immunoreactive neurones (fig. 5A) and showed partial colocalisation with NOS-positive neurones (fig. 5B), in both areas. GPR30 neurones were far more numerous in the vlPAG (fig. 6C) than in the dlPAG (fig. 6B), but in both zones the numbers were significantly decreased in OVX compared to proestrus females, resulting in numbers of immunoreactive neurones similar to the numbers found in males (fig. 6B, C). The proportion of NOS-positive neurones displaying GPR30-LI was similarly decreased in OVX (table 1). On sections at similar levels, GPR30 labelling was present in the large mesencephalic trigeminal neurones, while more ventrally immunoreactivity was observed in the dorsal raphe nucleus (DR), Edinger-Westfal nucleus (EW), parapontine tegmental nucleus (PPTg), laterodorsal tegmental nucleus (LDTg), cochlear nucleus, ventral tegmental area (VTA), substantia nigra (SN) and pontine nucleus (Pn). In these areas, variable numbers of GPR30-positive neurones were observed that often coexpressed ChAT (EW and LDTg; fig. 5C), NOS (LDTg, PPTg and DR), 5-HT (DR) and TH (VTA and SN).

Medulla Oblongata

In the NTS and VLM, colocalisation of GPR30-LI was found in 30–40% of cells expressing NOS (fig. 5E; table 1). Neurones of the catecholaminergic groups showed variable levels of GPR30-LI, for example in most A2 neurones of the NTS (fig. 5D) and subpopulations of A1 and C1 neurones in the VLM (fig. 5G; table 1). The numbers of immunoreactive neurones in both the NTS and RVLM appeared slightly increased in OVX females compared to

metoestrus and proestrus (fig. 6D, E), but not significantly so except for the VLM (p < 0.01 vs. metoestrus), which also contained higher numbers of neurones with GPR30-LI in males (fig. 6E). The proportion of TH-positive neurones was increased in OVX compared to metoestrus females (p < 0.05; table 1). Distinct GPR30 labelling was seen in almost all the large, cholinergic neurones of the DVN and NAmb and generally in the cranial motor nuclei (e.g. NAmb; fig. 5F) partial coexpression of GPR30-LI with ChAT was evident. In other areas of the medulla, large neurones of the intensely labelled type were prominent in the raphe magnus (RM), raphe pallidus (RPa), gigantocellular (Gi) and parapyramidal (pPyr) reticular areas of the ventromedial medulla (fig. 3A, 5H) with GPR30-LI present in the majority of 5-HT-positive neurones in these areas (fig. 5I).

Discussion

The results presented here confirm expression of GPR30 in neurones of several autonomic nuclei of the rat brain using quantitative real-time PCR and immunofluorescence labelling. While GPR30 has already been localised in neurones of some of these brain areas using immunohistochemistry [20, 21, 33, 34], the levels of protein expression have not been investigated. Furthermore, previous studies looking at GPR30 mRNA expression in the rodent [21, 22, 35] focused on only a few selected brain areas in animals at specific stages of the oestrous cycle and following ovariectomy. Our study is the first to examine the mRNA expression in key autonomic nuclei over the entire oestrous cycle and in OVX animals. At the same time, we have performed a quantitative analysis of GPR30-LI in these areas using stereological methodology based on a novel application of confocal imaging. Our findings indicate that changes in GPR30 expression might occur in areas of the rat brain associated with central autonomic control in response to fluctuations in oestrogen levels over the oestrous cycle.

Our PCR and immunohistochemistry data suggest that neurones expressing GPR30 are similarly distributed in areas of the hypothalamus and medulla oblongata in age-matched female and male rats. This is in agreement with other studies that reported no gender differences in the pattern of GPR30 expression [20, 36]. However, when we examined the expression levels of males and females at different stages of the oestrous cycle, we found that GPR30 mRNA levels in male rats were comparable to those of the metoestrus female rats but were considerably

Table 1. Colocalisation of GPR30-LI in NOS-, TH- and VP-immunoreactive neurones in autonomic areas of the rat brain (mean ± SE, n = 5)

Brain area	Neurone type	Proportion (%) of neurones displaying GPR30-LI		
		metoestrus	proestrus	OVX
PVN	NOS	58.7 ± 5.1*	64.1 ± 2.0##	41.04 ± 3.3*, ##
	TH	ND	ND	ND
	VP	40.9 ± 4.2	41.0 ± 3.3	37.7 ± 2.5
PAG				
Dorsolateral	NOS	49.7 ± 2.7	55.7 ± 1.7**	42.9 ± 2.7**
Ventrolateral	NOS	47.8 ± 1.7	51.6 ± 1.9	48.4 ± 1.4
	TH	ND	ND	ND
VLM	NOS	54.1 ± 3.6	59.4 ± 5.2	63.6 ± 3.6
	TH	53.3 ± 2.1*, #	63.1 ± 1.9#	66.7 ± 2.2*
NTS	NOS	35.4 ± 3.1	43.1 ± 4.9	30.9 ± 2.5
	TH	71.5 ± 1.4	72.5 ± 2.1	76.1 ± 3.3

ND = Not determined by quantitative analysis: GPR30-positive neurones are present in the same area, but very few (<5%) of the cells show double labelling.
* and # – difference between values marked at p < 0.05.
** and ## – difference between values marked at p < 0.01.

lower than the levels seen in the proestrus and oestrus females. The numbers of neurones showing GPR30-LI tended to be lower in males in most brain areas examined except the VLM, as revealed by quantitative immunohistochemistry, which we assume to give a rough indication of overall protein expression levels of GPR30.

It has already been shown that the expression of the classical ERα subtype changes in response to the levels of circulating oestrogen in many areas of the rat brain including the Arc, VMH and preoptic hypothalamus [24, 26, 37] and the NTS [27]. In examining expression in the PAG, NTS and VLM over the 4 stages of the oestrous cycle, we found significant changes in GPR30 mRNA levels, with the lowest levels observed during metoestrus, when oestrogen levels are low. Expression then increased over the cycle with greater expression in proestrus, when oestrogen is at its highest, peaking during oestrus when oestrogen levels fall again. These results suggest that GPR30 mRNA expression might be regulated by the levels of circulating gonadal steroids. However, while there seems to be a correlation between low oestrogen levels and low levels of GPR30 mRNA and vice versa it should be noted that GPR30 expression does not appear to decline dramatically after ovulation when oestrogen levels

fall in oestrus. This may reflect a delay in the response as a result of the time taken for the up- or down-regulation of mRNA production. The only previous study to report changes in GPR30 expression was performed in hamster ovarian cells, where they reported increased mRNA and protein levels during dioestrus [28]. In in vitro systems, stimulation of transfected cell lines with oestradiol has been shown to cause translocation of GPR30 from the cell membrane into the cytoplasm [19, 38].

Variations in HR, BP, baroreceptor reflex sensitivity (BRS) and cardiac autonomic activity have been observed in intact female rats over the oestrous cycle [13, 14] and hypertension is known to develop following ovariectomy, after an initial fall in BP and BRS in the first 1–2 weeks [12, 13]. Phases of the cycle when oestrogen levels are high are associated with increases in mean arterial BP and BRS and these variations are abolished following ovariectomy [11, 13, 39]. Numerous studies have shown oestrogen to have a modulatory effect on autonomic outflow and baro-reflex function [23, 40]. Increases in parasympathetic tone and BRS were observed following bilateral injection of oestrogen into the NTS and NAmb [3, 4], whereas sympathetic tone was significantly decreased following injection into the NTS and VLM [4]. If these responses are due to the activation of ERs in these areas, then it is possible that the beneficial effects may be due in part to rapid, non-transcriptional oestrogenic actions via GPR30. A recently generated GPR30 knockout mouse model displays increased BP, hyperglycemia and impaired glucose tolerance, and reduced body growth [35] but shows no impairment of reproductive function [41]. This suggests that GPR30 may have functional roles distinct from the classical ERs, concerned with homeostatic/autonomic regulatory, rather than reproductive processes.

OVX animals were maintained for 3 weeks following surgery before GPR30 mRNA expression levels were assessed: at this time point the changes in BP, HR and BRS are expected to be established and stable [11, 12]. The effects of oestrogen removal on the expression of GPR30 varied between the brain areas analysed. In the medullary nuclei (NTS and VLM), GPR30 mRNA appeared to be increased in OVX rats compared to the sham-operated controls. However, in contrast, in the PVN of the hypothalamus and the midbrain PAG, the levels of GPR30 mRNA expression appeared decreased. This suggests different mechanisms regulating GPR30 expression in different brain regions, with either differential sensitivity of neurones to circulating oestrogen levels, or other regulatory factors having an overriding importance in certain

brain areas. The non-genomic regulation of neural activity by oestrogen is highly complex and is also dependent on local aromatase enzyme activity, which is in turn influenced by circulating hormone levels [1, 42]. Groups of aromatase-positive neurones have been reported in broadly the same areas of the avian and mammalian brain, including the PVN, PAG and NTS as those in which we describe GPR30 neurones [43, 44].

The distribution of GPR30-LI within the brain supports the PCR data and indicates expression of the receptor protein in neurones in nuclei or areas known to be concerned with autonomic regulation, including the PVN, PAG, NTS and VLM. Quantitative immunohistochemistry to assess the numbers of neurones displaying GPR30-LI in these areas generally confirmed the changes in expression in OVX animals observed with PCR. Dual labelling studies suggested that GPR30 is not expressed predominantly in any one particular neuronal phenotype; for example in different areas of the medulla, coexistence could be variously observed in TH-positive catecholaminergic neurones (e.g. NTS and VLM), ChAT-positive cholinergic neurones (e.g. DVN, cranial motor nuclei), NOS-positive nitrergic neurones (PVN, NTS, PAG) and 5-HT-positive serotonergic neurones (raphe nuclei). The very prominent, strongly GPR30-immunoreactive gigantocellular neurones within the rostral ventromedial medulla were mostly separate from NOS and 5-HT-positive cells. This region is known to have extensive reciprocal connections with many brain areas, such as the hypothalamus and PAG and the spinal cord [45] and is associated with autonomic functions, including thermogenesis [46] and antinociception [47]. In the hypothalamic PVN, known to have important roles in functions influenced by oestrogen such as reproductive behaviour, body fluid homeostasis and BP regulation, particularly through regulating sympathetic activity in response to stress [48], GPR30-LI was observed in subpopulations of VP and NOS-immunoreactive neurones. This is contrary to the findings of an earlier study on 10-week-old male and female Sprague-Dawley rats that detected GPR30 only in oxytocin neurones of the PVN [21]. In the PAG, neurones showing GPR30-LI were mostly separate from the NOS-immunoreactive population and were far more numerous in the sympathoinhibitory ventrolateral column [9, 49]. However, a similar decrease in GPR30-LI was seen in the dorsolateral PAG, the 'hypertensive' area associated with the defence reaction [10].

Other neurones displaying GPR30-LI, for example those in the posterodorsal thalamus (overlapping the PVP and PrC), fall outside recognised anatomical or

functional divisions of the brain, and so their significance remains to be established. There is a question as to whether these cells might actually belong to the rostral-most extension of the PAG; however, neuronal tracing studies have demonstrated that this area of the thalamus is a target of extensive axonal projections from PAG neurones [50]. A further rather unexpected and potentially interesting finding was the presence of aggregations of GPR30-LI in the neuropil and small cells scattered along the subependymal layer of the third ventricle (e.g. mammillary recess) and within the circumventricular organs, where the blood-brain barrier is lacking (e.g. the SFO and SCO). This has not been previously reported, but may indicate a role for GPR30 in mediating the actions of oestrogen on transport and exchange between brain tissue, the blood and the cerebrospinal fluid that warrants further investigation. The circumventricular organs may offer a further route by which oestrogen is capable of exerting generalised central actions concerned with bodily homeostasis, behaviour and neuronal development [51].

Our investigation of the subcellular distribution of GPR30-LI within neurones revealed a high degree of co-localisation with TGN38, indicating a localisation mainly within the Golgi system, in agreement with the findings of previous studies using different GPR30 antisera [21, 22]. This predominantly intracellular localisation in neurones does not necessarily rule out a functional receptor role for GPR30 expressed at the plasmalemma. It may be that the antibodies we used preferentially recognise a precursor form of GPR30 or when inserted into the plasmalemma the mature receptor is modified in some way that impairs recognition. As GPR30 has been localised to the cell membrane in transfected cells [17, 19, 52], this may indicate that the concentration of receptor present at the cell membrane is normally below the threshold of immunohistochemical detection. Alternatively, since gonadal steroids can freely diffuse through cell membranes, GPR30 could fulfil a receptor role by interaction with oestrogen on membranes of the Golgi apparatus.

The variations in GPR30 expression levels over the oestrus cycle and following ovariectomy suggest that its regulation may be under the influence of circulating oestrogen levels. This combined with its presence in areas of the brain involved in autonomic regulation, in particular the pathways of baroreflex control may have direct consequences for the regulation of autonomic tone and baroreflex sensitivity, for example when the oestrogen levels decline following menopause. However, these results only provide a limited insight into what is a highly complex pattern of oestrogen signalling throughout the rat brain, which appears to have a high degree of regional specificity.

Acknowledgement

References

1 Cornil CA, Ball GF, Balthazart J: Functional significance of the rapid regulation of brain estrogen action: where do the estrogens come from? Brain Res 2006;1126:2–26.
2 Maggi A, Ciana P, Belcredito S, Vegeto E: Estrogens in the nervous system: mechanisms and nonreproductive functions. Annu Rev Physiol 2004;66:291–313.
3 Saleh MC, Connell BJ, Saleh TM: Autonomic and cardiovascular reflex responses to central estrogen injection in ovariectomized female rats. Brain Res 2000;879:105–114.
4 Saleh MC, Connell BJ, Saleh TM: Medullary and intrathecal injections of 17β-estradiol in male rats. Brain Res 2000;867:200–209.
5 Saleh TM, Connell BJ, Saleh MC: Acute injection of 17β-estradiol enhances cardiovascular reflexes and autonomic tone in ovariectomized female rats. Auton Neurosci 2000;84:78–88.
6 Spyer KM: Central nervous mechanisms contributing to cardiovascular control. J Physiol (Lond) 1994;474:1–19.

7 Loewy AD: Central autonomic pathways; in Loewy AD, Spyer KM (eds): Central Regulation of Autonomic Functions. New York, Oxford University Press, 1990, pp 88–103.
8 Dampney RA, Horiuchi J, Killinger S, Sheriff MJ, Tan PS, McDowall LM: Long-term regulation of arterial blood pressure by hypothalamic nuclei: some critical questions. Clin Exp Pharmacol Physiol 2005;32:419–425.
9 Lovick TA: The periaqueductal gray-rostral medulla connection in the defence reaction: efferent pathways and descending control mechanisms. Behav Brain Res 1993;58:19–25.
10 Carrive P: The periaqueductal gray and defensive behavior: functional representation and neuronal organization. Behav Brain Res 1993;58:27–47.
11 Takezawa H, Hayashi H, Sano H, Saito H, Ebihara S: Circadian and estrous cycle-dependent variations in blood pressure and heart rate in female rats. Am J Physiol 1994; 267:R1250–R1256.

12 Sasaki T, Ohno Y, Otsuka K, Suzawa T, Suzuki H, Saruta T: Oestrogen attenuates the increases in blood pressure and platelet aggregation in ovariectomized and salt-loaded Dahl salt-sensitive rats. J Hypertens 2000;18: 911–917.
13 Goldman RK, Azar AS, Mulvaney JM, Hinojosa-Laborde C, Haywood JR, Brooks VL: Baroreflex sensitivity varies during the rat estrous cycle: role of gonadal steroids. Am J Physiol Regul Integr Comp Physiol 2009; 296:R1419–R1426.
14 Kuo TBJ, Lai CT, Hsu F-C, Tseng Y-J, Li JY, Shieh S-C, Tsai CJ, Yang CCH: Cardiac neural regulation oscillates with the estrous cycle in freely moving female rats: the role of endogenous estrogen. Endocrinology 2010; 151:2613–2621.
15 Spary EJ, Maqbool A, Batten TF: Oestrogen receptors in the central nervous system and evidence for their role in the control of cardiovascular function. J Chem Neuroanat 2009;38:185–196.

16 Pietras RJ, Szego CM: Specific binding sites for oestrogen at the outer surfaces of isolated endometrial cells. Nature 1977;265:69–72.

17 Thomas P, Pang Y, Filardo EJ, Dong J: Identity of an estrogen membrane receptor coupled to a G protein in human breast cancer cells. Endocrinology 2005;146:624–632.

18 Revankar CM, Cimino DF, Sklar LA, Arterburn JB, Prossnitz ER: A transmembrane intracellular estrogen receptor mediates rapid cell signaling. Science 2005;307:1625–1630.

19 Funakoshi T, Yanai A, Shinoda K, Kawano MM, Mizukami Y: G protein-coupled receptor 30 is an estrogen receptor in the plasma membrane. Biochem Biophys Res Commun 2006;346:904–910.

20 Brailoiu E, Dun SL, Brailoiu GC, Mizuo K, Sklar LA, Oprea TI, Prossnitz ER, Dun NJ: Distribution and characterization of estrogen receptor G protein-coupled receptor 30 in the rat central nervous system. J Endocrinol 2007;193:311–321.

21 Sakamoto H, Matsuda K, Hosokawa K, Nishi M, Morris JF, Prossnitz ER, Kawata M: Expression of G protein-coupled receptor-30, a G protein-coupled membrane estrogen receptor, in oxytocin neurons of the rat paraventricular and supraoptic nuclei. Endocrinology 2007;148:5842–5850.

22 Matsuda K, Sakamoto H, Mori H, Hosokawa K, Kawamura A, Itose M, Nishi M, Prossnitz ER, Kawata M: Expression and intracellular distribution of the G protein- coupled receptor 30 in rat hippocampal formation. Neurosci Lett 2008;441:94–99.

23 Spary EJ, Maqbool A, Batten TFC: Oestrogen receptors in the central nervous system and evidence for their role in the control of cardiovascular function. J Chem Neuroanat 2009;38:185–196.

24 Zhou Y, Shughrue PJ, Dorsa DM: Estrogen receptor protein is differentially regulated in the preoptic area of the brain and in the uterus during the rat estrous cycle. Neuroendocrinology 1995;61:276–283.

25 Haywood SA, Simonian SX, van der Beek EM, Bicknell RJ, Herbison AE: Fluctuating estrogen and progesterone receptor expression in brainstem norepinephrine neurons through the rat estrous cycle. Endocrinology 1999;140:3255–3263.

26 Shughrue PJ, Bushnell CD, Dorsa DM: Estrogen receptor messenger ribonucleic acid in female rat brain during the estrous cycle: a comparison with ovariectomized females and intact males. Endocrinology 1992;131:381–388.

27 Spary EJ, Maqbool A, Batten TFC: Changes in oestrogen receptor expression in the nucleus of the solitary tract of the rat over the oestrus cycle and following ovariectomy. J Neuroendocrinol 2010;22:492–502.

28 Wang C, Prossnitz ER, Roy SK: Expression of G protein-coupled receptor 30 in the hamster ovary: differential regulation by gonadotropins and steroid hormones. Endocrinology 2007;148:4853–4864.

29 Spary EJ, Chapman SE, Maqbool A, Batten TFC: Novel oestrogen receptor GPR30: brain localisation and changes in expression during the rat oestrus cycle. Auton Neurosci 2007;135:61–62.

30 Saha S, Spary EJ, Maqbool A, Asipu A, Corbett EK, Batten TF: Increased expression of AMPA receptor subunits in the nucleus of the solitary tract in the spontaneously hypertensive rat. Brain Res Mol Brain Res 2004;121:37–49.

31 Paxinos G, Kus L, Ashwell KWS, Watson C: Chemoarchitectonic Atlas of the Rat Forebrain, ed 1. San Diego, Academic Press, 1999.

32 Paxinos G, Carrive P, Wang H, Wang P-Y: Chemoarchitectonic atlas of the rat brainstem, ed 1. San Diego, Academic Press, 1999.

33 Xu H, Qin S, Carrasco GA, Dai Y, Filardo EJ, Prossnitz ER, Battaglia G, DonCarlos LL, Muma NA: Extranuclear estrogen receptor GPR30 regulates serotonin function in rat hypothalamus. Neuroscience 2009;158:1599–1607.

34 Hazell GG, Yao ST, Roper JA, Prossnitz ER, O'Carroll AM, Lolait SJ: Localisation of GPR30, a novel G protein-coupled oestrogen receptor, suggests multiple functions in rodent brain and peripheral tissues. J Endocrinol 2009;202:223–236.

35 Mårtensson UE, Salehi SA, Windahl S, Gomez MF, Swärd K, Daszkiewicz-Nilsson J, Wendt A, Andersson N, Hellstrand P, Grände PO, Owman C, Rosen CJ, Adamo ML, Lundquist I, Rorsman P, Nilsson BO, Ohlsson C, Olde B, Leeb-Lundberg LM: Deletion of the G protein-coupled receptor 30 impairs glucose tolerance, reduces bone growth, increases blood pressure, and eliminates estradiol-stimulated insulin release in female mice. Endocrinology 2009;150:687–698.

36 Dun SL, Brailoiu GC, Gao X, Brailoiu E, Arterburn JB, Prossnitz ER, Oprea TI, Dun NJ: Expression of estrogen receptor GPR30 in the rat spinal cord and in autonomic and sensory ganglia. J Neurosci Res 2009;87:1610–1619.

37 Simerly RB, Carr AM, Zee MC, Lorang D: Ovarian steroid regulation of estrogen and progesterone receptor messenger ribonucleic acid in the anteroventral periventricular nucleus of the rat. J Neuroendocrinol 1996;8:45–56.

38 Filardo E, Quinn J, Pang Y, Graeber C, Shaw S, Dong J, Thomas P: Activation of the novel estrogen receptor G protein-coupled receptor 30 (GPR30) at the plasma membrane. Endocrinology 2007;148:3236–3245.

39 Goldman RK, Azar AS, Mulvaney JM, Brooks VL: Baroreflex sensitivity varies during the estrus cycle of the rat. FASEB J 2008;22:941.12.

40 Saleh TM, Connell BJ: Role of oestrogen in the central regulation of autonomic function. Clin Exp Pharmacol Physiol 2007;34:827–832.

41 Otto C, Fuchs I, Kauselmann G, Kern H, Zevnik B, Andreasen P, Schwarz G, Altmann H, Klewer M, Schoor M, Vonk R, Fritzemeier KH: GPR30 does not mediate estrogenic responses in reproductive organs in mice. Biol Reprod 2009;80:34–41.

42 Cornil CA, Charlier TD: Rapid behavioural effects of oestrogens and fast regulation of their local synthesis by brain aromatase. J Neuroendocrinol 2010;22:664–673.

43 Sanghera MK, Simpson ER, McPhaul MJ, Kozlowski G, Conley AJ, Lephart ED: Immunocytochemical distribution of aromatase cytochrome P450 in the rat brain using peptide-generated polyclonal antibodies. Endocrinology 1991;129:2834–2844.

44 Evrard HC, Harada N, Balthazart J: Immunocytochemical localization of aromatase in sensory and integrating nuclei of the hindbrain in Japanese quail (Coturnix japonica). J Comp Neurol 2004;473:194–212.

45 Hermann DM, Luppi PH, Peyron C, Hinckel P, Jouvet M: Afferent projections to the rat nuclei raphe magnus, raphe pallidus and reticularis gigantocellularis pars alpha demonstrated by iontophoretic application of choleratoxin (subunit b). J Chem Neuroanat 1997;13:1–21.

46 Morrison SF, Nakamura K, Madden CJ: Central control of thermogenesis in mammals. Exp Physiol 2008;93:773–797.

47 Heinricher MM, Tavares I, Leith JL, Lumb BM: Descending control of nociception: specificity, recruitment and plasticity. Brain Res Rev 2009;60:214–225.

48 Kenney MJ, Weiss ML, Haywood JR: The paraventricular nucleus: an important component of the central neurocircuitry regulating sympathetic nerve outflow. Acta Physiol Scand 2003;177:7–15.

49 Dean C: Sympathoinhibition from ventrolateral periaqueductal gray mediated by the caudal midline medulla. Am J Physiol Regul Integr Comp Physiol 2005;289:R1477–R1481.

50 Krout KE, Loewy AD: Periaqueductal gray matter projections to midline and intralaminar thalamic nuclei of the rat. J Comp Neurol 2000;424:111–141.

51 Curtis KS: Estrogen and the central control of body fluid balance. Physiol Behav 2009;97:180–192.

52 Filardo EJ, Thomas P: GPR30: a seven-transmembrane-spanning estrogen receptor that triggers EGF release. Trends Endocrinol Metab 2005;16:362–367.